Drag on Bluff and Streamlined Bodies

Laboratory Experiment
ME 608 Fluid Dynamics, Fall 2018

TECHNICAL REPORT

December 2018

Name of Group Members

Charlie Nitschelm
Author One, cjn1012@wildcats.unh.edu

Ross Thyne
Author Two, rdt1002@wildcats.unh.edu

Joseph Williams
Author Three, jmw1019@wildcats.unh.edu

Lab Section: 3

Lab Time: Tues, 12/4, 3:10-4:30 (3)

Department of Mechanical Engineering
University of New Hampshire

Professor M. Wosnik
Teaching Assistants:
J. Cuevas Bautista, C. Boahmah-Mensah

Table of Contents

List of Figures

List of Tables

Abstract

A drag analysis on three separate objects was conducted at the University of New Hampshire's wind tunnel located in Kingsbury Hall. The three objects, a square cylinder, a sphere cylinder and a NACA 0020 airfoil, were constrained inside the test section of the wind tunnel. A pressure differential was applied to the wind tunnel to begin airflow across each of these objects in the test section so measurements could be recorded to determine which shapes were most effective to limit the drag force applied to the object. The NACO 0020 airfoil was the most effective to limit drag, with the circular cylinder and square cylinder following it, respectively. Tests were also conducted on the square cylinder by adding tape to the top and bottom of the cross section impeding the flow to determine how it would affect its drag characteristics.

Introduction and Background

Fluid dynamic drag rose in popularity during the dawn of the 20th century as humans began to take to the air with the invention of the first airplane. Since then, the field of fluid dynamic drag has been crucial to all dynamic inventions since. The interactions between fluid particles and rigid bodies continue to be studied to obtain a better understanding on how these objects behave in flight on Earth with an atmosphere. These studies have helped us create designs to behave appropriatly based on the application it is used in.

These applications can be understood from a casual trip on a commercial airplane. During takeoff, we seek to reach a speed in order to maximize its lift force to rise off the ground, and during landing, we seek to maximize drag to slow down the airplane to a safe landing speed once again. Drag impedes objects motion by stealing momentum from the body and transferring it to the molecules it encounters.

Theory

Forces imparted on and object are completely dependent on the properties of the body and the fluid it is encountering. It does not matter if the body is moving through a static fluid, or a fluid is rushing past a static body, the drag it experiences is completely dependent on the relative speed of the body and the fluid. These are referred to as mobile fluid dynamic drag and static fluid dynamic drag, respectively.

A flow field helps us understand fluid motion more directly. To calculate a flow field, we must understand the velocity of the encountering flow at various points around the immersed object. Normal and tangential stresses can be used to calculate the flows and flow gradients over the immersed body's surface from the following equation:

$$\vec{F}_{res} = \iint_{CS} \vec{t}\, dS = \iint_{CS} \vec{n} \cdot \bar{\bar{T}}\, dS \qquad (1)$$

Non-dimensional quantitative values can be collected through an fluids experiment which can then be used in modeling as similar shapes often have close drag coefficients to the Reynolds Number. The equation below describes the basic equation of objects in external flows:

$$Re = \frac{\rho V l}{\mu} \tag{2}$$

where ρ is the density of the fluid, V is the velocity of the fluid in relation to the object, l is the characteristic length or the chord width of an airfoil, and μ is the dynamic viscosity of the fluid. Buckingham Pi Theorem allows us to view the drag force and the coefficient of drag in terms of the Reynolds Number of the experiment setup. The equation below, which relates the force of drag, F_D, with the Reynolds number, is used to understand how the coefficient of drag related to its Reynolds number.

$$\frac{F_D/L}{D\rho U_c^2} = \varphi\left(\frac{\rho U_c L_c}{\mu}\right) \quad \Downarrow \quad c_D = f(Re) \tag{3}$$

Experimental Setup

The experimental wind tunnel in Kingsbury Hall at the University of New Hampshire is a laboratory design, Model 404B(Canvas). The 3 objects tested, which have fundamentally different shapes, are characterized in the table below detailing the shape parameters and its material.

Table 1: Significant dimensions of the test shapes

Shape	Material	Diameter (mm)	Length (mm)	Chord (mm)
Square Cylinder	Aluminum 6061	25.65	457.2	N/A
Round Cylinder	Aluminum 6061	60.45	455.61	N/A
Airfoil	Aluminum 6061	27.63	454	138.18

The ELD 440B wind tunnel is equipped with an 18” x 18” x 36” test section volume. Below is a table that details the blockage ratio or the flow-facing area of the body cross section to the cross-section area of the test section.

Table 2: Blockage ratio of each shape

Shape	Blockage (%)
Square Cylinder – Diameter	5.60
Round Cylinder – Diameter	5.55
Airfoil – Diameter	6.06
Airfoil – Chord	6.00

There are three apparatuses that were implemented to help in measuring the physical quantities during the test. A force balance, pitot-static tube and manometers enabled us to make the calculations necessary to accurately model its characteristics during the flow tests. The force balance allowed us to measure the force of drag on the body using a balance mounted in the wind tunnel test area. Each shape was mounted the same way to maintain consistency in setup. The manometers measured the gage pressure during the test which assisted in verifying the actual flow velocity by obtaining its data by being tangential to the flow. The pitot-static tube did the same calculation but differed by directly facing the flow.

Physical measurements were also made outside of the test sections including the physical quantities of the body, like length, diameter, and chord length. Real-time fluid properties must be measured and recorded to ensure accuracy of data. The viscosity and air density of the fluid through the test section were measured with respect to its temperature as these properties are directly related to the measurements being taken.

Table 3: Density and viscosity of the flow fluid with temperature

Kingsbury Hall S125	Temperature [°C]	ρ_{air} $[kg/m^3]$	μ_{air} $[Ns/m^2]$
Beginning of Lab (15:24)	24	1.188	$1.832*10^{-5}$
Middle of Lab (15:54)	24.9	1.184	$1.836*10^{-5}$
End of Lab (16:24)	25	1.183	$1.837*10^{-5}$

During the test, we experienced a temperature increase of a few degrees Celsius as the bodies and the devices performing the test send out a significant amount of thermal energy. These fluid properties through the time of the experiment were calculated by proven table depending on the temperature of the fluid. The measurement sections were completed by having students take initial measurements of each of the shapes as these will be important for post analysis. They were measured multiple times and averaged to obtain an accurate result.The installation/preparation stage consisted of learning how to handle the ELD 404B wind tunnel. Each of the shapes were placed into the test section paying close attention to make sure the body was not touching the walls, leaving a small gap to make sure none of the drag force would be transferred into the wall, and not the force balance. The operations/measurement stage happened multiple times to get the data from each of the shapes tested. The square body was tested first, oriented to have a flat face perpendicular to the flow. The round cylinder was tested next, making sure the fixture of the body was set up the same as the square. We then tested the NACA 0020 airfoil at a zero angle of attack with respect to the flow field.

Once the three shapes were tested, we went back to the round cylinder shape and added strips of tape to the bottom and top of the cross section against the flow field, acting as a flow trip disrupting the laminar flow it experiences around it. During all these tests, values were recorded for drag force and manometer readings. The drag force readings were the instantaneous values read from the force balance, and the manometer was read by eye from a resting fluid.

There were various sources of error during the test that could affect our final calculations. All physical measurement of the objects are not perfect and are subject to human error of up to 1 millimeter. Our

tests are also subject to error as the flow velocity rose to higher values, the bodies could collide with the wall, imparting some of the drag force into the wall, lowering the actual drag the body is encountering recorded from the force balance. When setting the airfoil and square into the holding apparatus, there was also no direct certainty in the angular orientation with relation to the flow direction, which could have effects on our results for drag.

Discussion of Results

From the wind-tunnel experiments, we covered Reynolds number values from 11,000 to 250,000. These experiments exemplified turbulent flows across the different shapes. The measured drag forces at a 0° angle of attack (AoA=0°) were plotted against the respective Reynolds number based on the cross-stream area, as shown in Figure 1. Analysis of these graphs show a quadratic trend to the data set, excluding the cylinder with tape, this is due to the force of drag being proportional to the velocity squared. The data also indicated that the NACA Airfoil was the most aerodynamic at an AoA=0° because it had lowest drag force at all Reynolds numbers, while the square had the highest drag force at each respective Reynolds number.

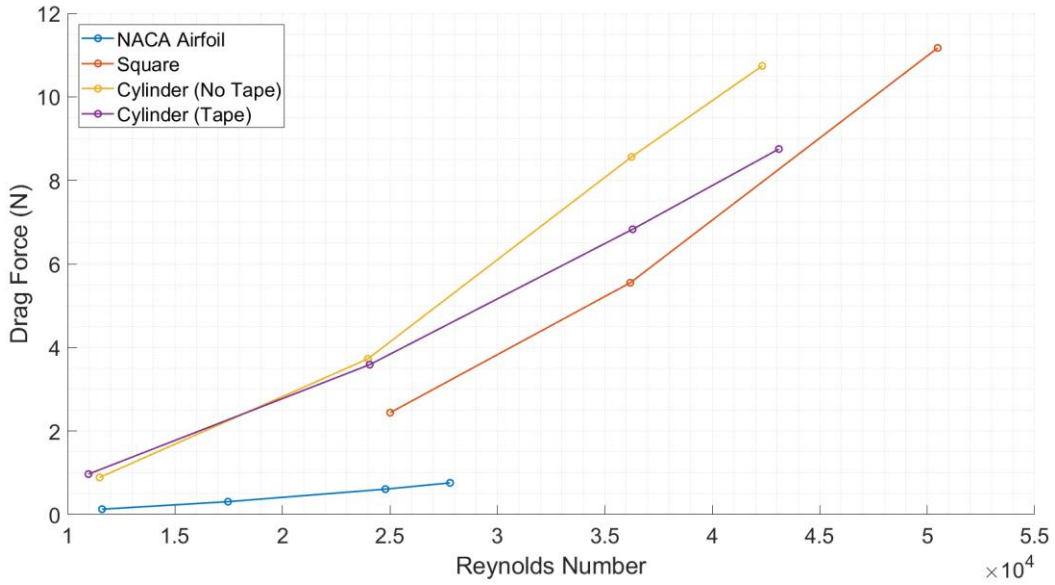

Figure 1. Drag Force, F_D [N], vs Reynolds number, Re_D, for circular and square cylinders and NACA 0020 airfoil.

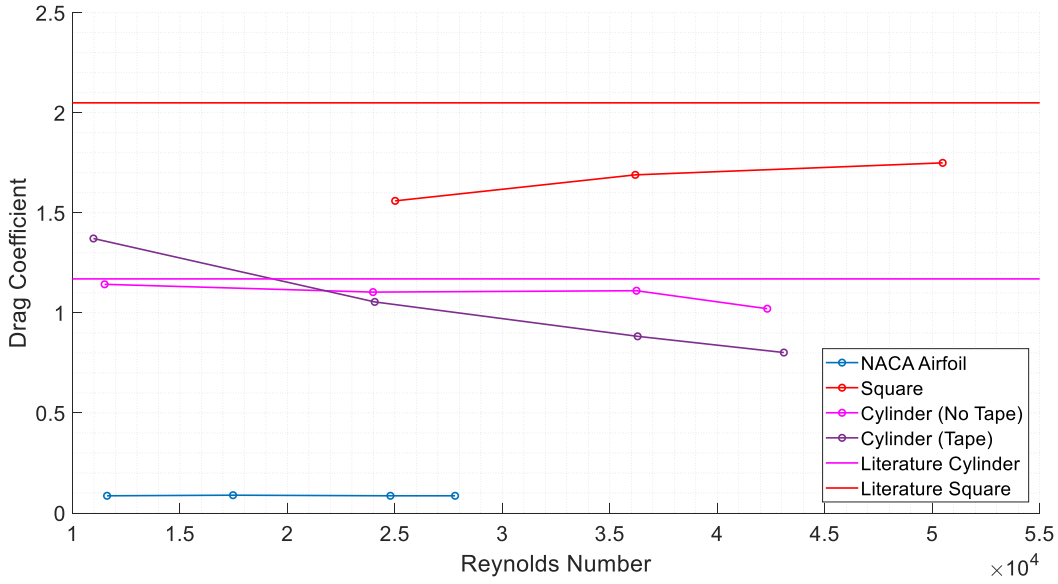

Figure 2. Drag coefficient, c_D, vs Reynolds number, Re_D, for circular and square cylinders and NACA 0020 airfoil, with comparison to values from literature.

Based on the values found from literature, our data does appear accurate. The cylinder slightly deviates below the literature values, and the cylinder with tape deviates even more as the addition of tape creates more turbulent flow, lowering the drag coefficient. Also, from the graph we can determine that the drag coefficient is relatively independent from Reynolds number. This details that our tests have variation that needs to be considered when using the actual data for real engineering solutions.

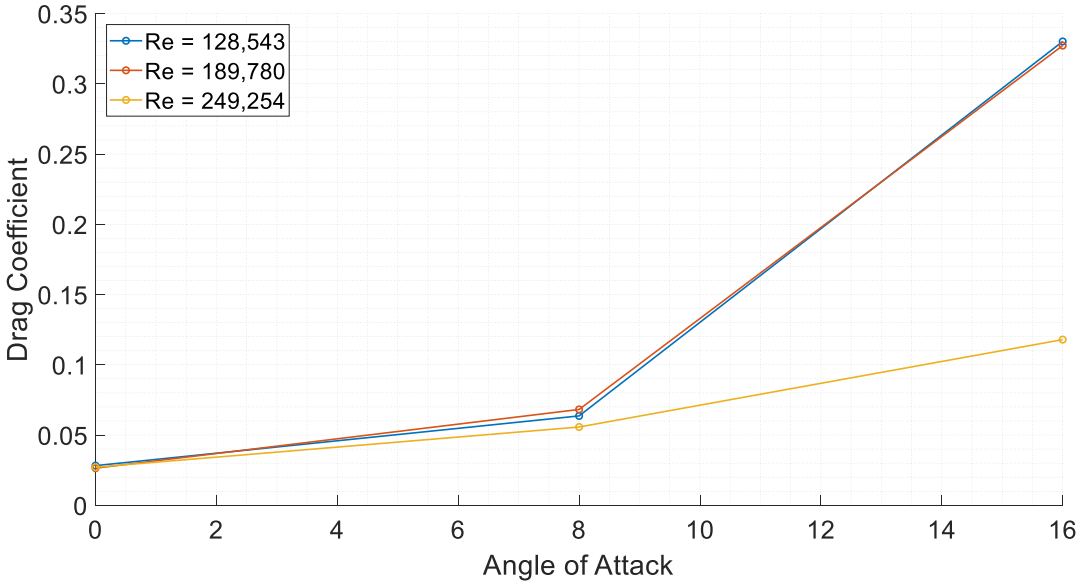

Figure 3. Drag coefficient, c_D, vs angle of attack, α, for three different Reynolds numbers for NACA 0020.

From this data we can see that with higher Reynolds numbers, or more turbulent flow, the coefficient of drag is lower than that of lower Reynolds numbers. This occurs because turbulent boundary layers are more resistent to separation than laminar boundary layers, so the flow stays attached to the airfoil longer, resulting in decreased form drag. It is also apparent that at the greater the angle of attack, the greater the coefficient of drag, at any Reynolds number.

Summary and Conclusion

Participating in a hands-on lab was crucial to our development to understand flow around an object when immersed in it. We calculated the actual relations between Reynolds Number, drag forces and the respective coefficient of drag. It allowed us to practice our skills in measuring, installing and operating the wind tunnel. The recordings from the experiment then enabled us to analyze and these relationships to get a better understanding of the complex field of fluid dynamics on moving bodies immersed in a fluid.

The wind tunnel allowed us to determine the basic properties of the drag on different objects. With respect to its drag force and drag coefficients, the NACA 0020 airfoil displaces the smallest values, which agrees with what we suspected as they are used on airplanes. The circular cylinder has the second smallest drag values, and then the square. When tape was added to the circular cylinder during our last test, the object experiences more drag during the low flow speeds, but then decreased compared to the object without tape, showing the phenomenon of how the fluid behaves at higher Mach numbers, preferring sharper objects against the flow, and allowing the flow to attach to the object for longer before splitting off of it, separating.

References

[1] S. F. Hoerner, Fluid-Dynamic Drag: practical information on aerodynamic drag and hydrodynamic resistance, Hoerner Fluid Dynamics, 1965.

[2] P. J. Pritchard, Fox and McDonald's Introduction to Fluid Mechanics, 8th edition, John Wiley & Sons, Inc., 2011.

[3] R. E. Sheldahl and P. C. Klimas, "Aerodynamic Characteristics of Seven Symmetrical Airfoil Sections Through 180-Degree Angle of Attack for Use in Aerodynamics Analysis of Vertical Axis Wind Turbines. Report SAND80-2114.," Sandia National Laboratories, 1981.